

Influence of composition and glass transition temperature on the diffusion and solubility behaviour of methyl ethyl ketone–isopropyl alcohol mixtures in poly(methyl methacrylate)

Richard A. Pethrick* and Kathleen E. Rankin

Department of Pure and Applied Chemistry, University of Strathclyde, 295 Cathedral Street, Glasgow, UK G1 1XL

Received 31st March 1998, Accepted 14th October 1998

The process of removal by a solvent mixture of low molar mass polymer generated as a consequence of chain scission is a critical step in electron beam lithography. The development of the image depends on a number of factors, including the composition of the solvent and the nature of the polymer. In this paper the effects of change in the composition of mixtures of methyl ethyl ketone and isopropyl alcohol, a common development solvent used in lithography, and the glass transition temperature of poly(methyl methacrylate) films on the mutual diffusion coefficient are reported. The mutual diffusion coefficient decreases and becomes asymmetric towards low volume fraction of solvent as the proportion of isopropyl alcohol in the mixture is increased. The higher glass transition temperature films are prone to exhibiting crazing on exposure to solvent. The diffusion of the mixture into the polymer film is selective and preferential for methyl ethyl ketone. Diffusion becomes complex as the content of the mixture moves towards a higher isopropyl alcohol composition. Also, there is evidence for both lowering of the glass transition temperature and re-precipitation of the polymer by the non-solvent (isopropyl alcohol). Change in the initial T_p of the films leads to small changes in the swelling rate. In the development process of electron beam resist films used in semiconductor lithography, crazing probably plays as important a role in the overall development process as simple solvent driven dissolution.

Introduction

The ability to achieve very large-scale integrated (VLSI) circuit fabrication depends critically on the precision of the lithographic processes used. While photolithography remains the primary tool for large-scale semiconductor fabrication, mask generation and specialist circuit fabrication is dominated by electron beam technology.¹ The lithography process is based on radiation induced changes in the dissolution rate of thin resist films. The type of development process is controlled by the nature of the interaction of the radiation with the resist, which may be to either degrade or crosslink the polymer. In general, there are several different regimes for polymer dissolution, each of which requires a separate model to describe the process. The mechanism for poly(styrene) dissolution in a good solvent is clearly very different from that for poly(methyl methacrylate) and both are different from the dissolution of the inhibited phenolic polymers used in photoresists.¹ Of these processes, only the first, dissolution of glassy amorphous polymers like poly(styrene), is reasonably well understood.^{2,3}

Peppas and co-workers have applied scaling concepts^{4,5} to the description of the dissolution of poly(styrene). Their theory assumes the initial formation of a gel layer at the polymer–solvent interface as the solvent diffuses into the film. Once this gel layer is formed, it propagates at constant thickness through the polymer film as dissolution occurs. The dissolution rate and thickness of the gel layer are dependent on the molecular weight of the polymer and are described accurately by reptation theory.⁵ Experiments on high molar mass poly(styrene) indicate that methyl ethyl ketone (MEK) dissolves at a rate predicted by theory, but these predictions failed when applied to poly(methyl methacrylate)^{6–8} (PMMA), where dissolution occurred without the formation of a significant gel layer.

Many electron beam resists are based on PMMA and development of the lithographic pattern is achieved by the use of mixtures of isopropyl alcohol (IPA) and MEK. Isopropyl alcohol is a non-solvent for PMMA, whereas MEK is a good solvent. During the exposure process, the high molar mass

polymer undergoes progressive scission producing a lower molar mass product. Changes in the solvent mixture and temperature result in the mixture changing from being a good to a poor solvent for the polymer. Since the solubility is a function of molar mass, it is possible to select a mixture which will selectively dissolve the low molar mass material without significantly swelling the unexposed, higher molar mass components. Despite the importance of electron beam lithography in VLSI fabrication, little research appears to have been carried out on the mechanism of polymer dissolution in these mixed solvent systems. PMMA can exist in three different stereochemical forms with different values of the T_g . Isotactic PMMA has a T_g of approximately 40°C, the atactic form has a T_g of 117°C and syndiotactic PMMA has a T_g of 125°C. The differences in the T_g values will also influence the solubility rates of polymers with the same molar mass.⁹ Differences in stereochemistry also influence the sensitivity of the polymer to electron beam irradiation.^{9–11} A combination of a more marked dependence of the solubility on molar mass for the isotactic polymer and changes in the distribution of the molar mass for the degraded polymer have a significant effect on the electron beam sensitivity. Ignoring slight differences in the degradation mechanism, the solubility rate of the exposed PMMA correlates well with the segmental mobility of the polymer. Changes in the size of the solvent used in the development process indicate that the solubility rates are strongly affected by the relative size of the interstitial distance (free volume) between the highly interpenetrating chain of the polymer and size of the solvent molecule. Plots of the solubility against molar mass of the solvent exhibit a sharp break in slope between propyl acetate and butyl acetate. The power dependence of the solubility on the molar mass between methyl acetate and propyl acetate is relatively weak, but between butyl acetate and the higher acetate homologues is very strong. For lower molar mass solvents there is relatively little correlation between the motion of the polymer chain and that of the solvent whereas, above propyl acetate, the motion is hindered by the polymer and a high degree of correlation

between the chain and solvent is required for diffusion. A typical development mixture, used in practice, consists of 1:3 MEK to IPA, at room temperature. Selection of the composition of the solvent mixture is usually based in measurement of dissolution rates. It has been shown that the dissolution rate (S) is related to the molar mass through eqn. (1),

$$S = KM^\alpha \quad (1)$$

where K and α are solvent dependent parameters that are specific to the particular polymer system under consideration.¹⁴ A number of instruments have been developed for the measurement of dissolution rates. The technique usually involves the measurement of changes in thickness of the resist layer, loss of weight or time to complete dissolution measured by end point analysis.¹⁵ However, these studies do not give a molecular interpretation of the dissolution process. A novel technique has been proposed¹⁶ which allows examination of the dissolution process by optical examination of the change that occurs in the optical interference, as a function of time, for micron thick films sandwiched into a Fabry Perot interferometer configuration.¹⁶ In this paper, the results of a study of the effects of solvent variation on the dissolution process for atactic PMMA are reported. The polymer selected is typical of the type of material commonly used in many electron beam resists.

Mixtures of MEK–IPA, in the range of 3:2 w/w MEK–IPA, are usually used for the development of electron beam resists. Compositions of 1:1, 3:2 and 31:9 w/w MEK–IPA were investigated in an earlier paper.¹⁶ It was observed that, as the amount of IPA is increased, the mutual diffusion coefficient was reduced. Also, it was noted this as the point at which the volume fraction of solvent coincides with the maximum mutual diffusion coefficient moves towards lower volume fractions of solvent in the films. In certain instances, the films exhibited environmental stress cracking, consistent with the good solvent (MEK) shocking the films' surface. This effect could be overcome simply by not baking the film, thus allowing the residual casting solvent to remain and to plasticise the film. A two stage diffusion process was also observed for certain compositions. In this paper, an attempt will be made to explore further the nature of the two stage diffusion process and to quantify the effect of baking on the properties of the films.

Experimental

Materials and thin film formation

Poly(methyl methacrylate) was obtained from Merck (Poole, UK), and had a nominal molar mass of $100\,000\text{ g mol}^{-1}$. The molar mass and its distribution were determined by gel permeation chromatography and a value of \bar{M}_n of $96\,000\text{ g mol}^{-1}$ and a heterogeneity index of 1.66 was obtained. Methyl ethyl ketone and isopropyl alcohol were used as solvents and were obtained from Merck (Poole, UK) as AnalaR grade reagents. The refractive indices of the solvent mixtures were measured using an Abbe refractometer. Films used in this study were spun onto chromium-coated glass substrates from a 3 wt% solution of polymer in MEK, using a Headway Research Incorporated spinner operating with speeds between 1000 and 500 revolutions per minute (rpm). $50\ \mu\text{l}$ of polymer solution were applied directly to the substrate ($2 \times 2\text{ cm}$). All solutions used were filtered through a $0.22\ \mu\text{m}$ filter prior to use. The best films were produced when 15 s was left between application of the droplet and spinning at a pre-set speed for 60 s.⁷ The films were baked at 120°C for 1 h to remove excess solvent and to aid development of a smooth profile. These films are of similar dimensions to those used in electron beam lithography.

Fabry Perot interferometer experiment for assessment of solvent diffusion

The basic interferometer used for assessment of the solvent diffusion process was constructed using two 6 mm thick glass plates which measured $25 \times 25\text{ mm}$. These were coated with chromium to achieve a transmission level of approximately 20%. The coating was carried out using an Edwards Coating System E306A and the transmission measured with a Perkin-Elmer 257 IR spectrometer. The polymer films were either spun coated onto the glass or, alternatively for thicker films, cast by slow evaporation from an 8 wt% solution in MEK. The film sandwiched between the plates was clamped using a normal IR plate holder. This construction was placed in a water jacket connected to a thermostatted bath and held at $30 \pm 0.1^\circ\text{C}$. A more detailed description of the experimental apparatus used has been published elsewhere.¹⁶ The fringe pattern was recorded using an Olympus CHC binocular microscope with an attached Olympus OM2 camera. The interferometer was illuminated with a sodium vapour lamp which has a strong band at 589 nm and the images recorded using a Kodak black and white Tri X Pan film which had a speed of 400 ASA and was sensitive to yellow light.

Operation of the Fabry Perot interferometer and data analysis

Solvent diffuses into the polymer, and the sharply defined edge of the film and the associated interference pattern becomes distorted, taking up a sigmoidal form which reflects the way in which the fringe pattern changes as the solvent diffuses into the polymer. Change in the number of fringes per unit dimension is a direct measure of the concentration–distance profile. This approach was initially proposed by Crank¹⁸ and by Crank and Park.¹⁹ Each interference fringe represents a plot of refractive index *versus* distance, over the concentration range from pure solvent to pure polymer. Assuming that the refractive index is linearly proportional to concentration and that there is negligible volume change on mixing of polymer and solvent, then the refractive index plot represents the concentration profile. The profiles were recorded at 3 min intervals and the fringes traced from the photograph. Where the fringe is horizontal at the film edge, the concentration of diffusing solvent is zero (*i.e.* $\phi_s = 0$) and where it is horizontal on the solvent side, the polymer concentration is zero (*i.e.* $\phi_s = 1.0$). The two measurable features are the change in the concentration profile and movement of the polymer film edge, which is a direct measure of the rate of swelling of the polymer film. When there is a discontinuity in the fringe pattern, which is a direct indication that the solvent is a poor solvent for the polymer (Fig. 1), then the maximum number of fringes, v_T , that would be observed between pure solvent and pure polymer is calculated using eqn. (2),^{18,19}

$$v_T = \frac{2l}{\lambda} (n_p - n_s) \quad (2)$$

where l is the film thickness, λ is the wavelength of the monochromatic light source and n_p and n_s are respectively the refractive indices for polymer and solvent. The mutual diffusion coefficient can be calculated using eqn. (3),^{18,19}

$$D_m = - \left(\frac{1}{2t} \right) \left(\frac{dx}{d\phi_s} \right)_{\phi_s = \phi_s'} \int_0^{\phi_s'} x d\phi_s \quad (3)$$

where ϕ_s is the volume fraction of solvent at some time t , at a plane distance x away from the original boundary between solvent and polymer. The original position of this boundary is always set in the same place. The Boltzmann transformation for any fixed value, ϕ_s , *versus* x/\sqrt{t} , for the data collected at

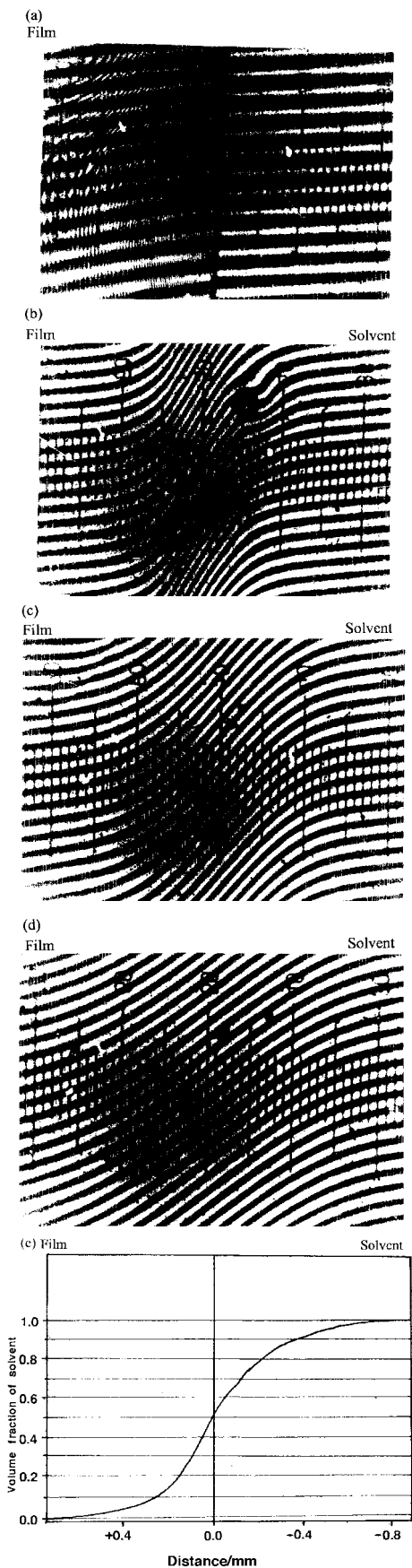


Fig. 1 Interference photographs for PMMA/MEK: (a) before solvent added, and after (b) 3, (c) 5 and (d) 10 min; (e) concentration–distance curve for PMMA/MEK.

various times should all fall on a single average curve if the process is Fickian.^{3,18,19} In this case, eqn. (3) gives eqn. (4).

$$D_m = - \left(\frac{1}{2} \right) \left(\frac{dx t^{\frac{1}{2}}}{d\phi_s} \right)_{\phi_s = \phi_s'} \int_0^{\phi_s'} x t^{\frac{1}{2}} d\phi_s \quad (4)$$

Gradient of tangent to the curve at ϕ_s' Area under the curve from 0 to ϕ_s'

This equation was used to calculate the concentration–distance profile for the system investigated.

Results and discussion

Secondary boundary phenomenon

Investigation of the diffusion behaviour with a 3:2 w/w IPA–MEK mixture showed that the curves up to about 16 min conformed to a simple one stage process. However, after 25 min a second boundary appeared at the edge close to the solvent and rapidly diffused into the film which already contained solvent. This was very marked at about 36 min, where it was observed that the second boundary had now reached a point about half way between the film surface and edge of the solvent diffusion front into the polymer. It is not possible to calculate a diffusion coefficient for the separate processes because it is not possible to determine the composition of the solvent mixture at the line between the two diffusion regions. In order to obtain an apparent mutual diffusion coefficient, an average value over the whole curve was calculated in the manner presented in the previous paper.¹⁶

Two hypotheses can be proposed to explain the observation of two diffusion regions.

Gel–glass boundary. It is possible that the feature is similar to that observed in poly(styrene),⁴ where a two stage diffusion process is associated with the solvent lowering the glass transition temperature. In the initial stages, the mixture diffuses into a glassy polymer and is controlled by the osmotic pressure–solubility of the solvent in the matrix. After sufficient solvent has diffused into the polymer matrix, the polymer is able to swell and changes from a glass into a gel state. In this initial stage, the solvent is diffusing into a mobile polymer state and diffusion is influenced by segmental motion and reptation of the polymer chains. Crank and Robinson²⁰ have termed this process middle boundary behaviour.

Preferential solvent absorption. When the solvent contains both good solvents and non-solvents, preferential absorption of the good solvent lowers the T_g . The expanded matrix allows access of the non-solvent which will reprecipitate the polymer and lead to the mixed solvent diffusion having a different rate to that of the initially absorbed good solvent. The second boundary is then associated with precipitation of polymer rather than the occurrence of the glass to gel transition.

In assessing the possible effects of the solvent on depression of the T_g , measurements using a penetration technique were made, as described previously.²¹ The apparatus consisted of a 6 mm diameter glass rod with a round tip at one end, which was allowed to rest on the sample which had been previously plasticised with a known composition of solvent. A chromel–alumel thermocouple was attached to the tip of the rod and the temperature measured using a Digitron 3750-K digital thermometer. A Shlumberger linear variable differential transducer (LVDT) was placed on the top of the probe and its movement recorded against temperature, using a two pen recorder. The sample was cooled with a methanol–cardice mixture or heated with a paraffin oil bath. The temperature

was changed at a rate of 3 K min⁻¹. The samples, in sealed phials, had been previously equilibrated for two days, in a temperature controlled oven at 40 °C, to allow the mixture to penetrate into the solid completely, and were cooled to room temperature, before the phials were opened, to avoid evaporation.

The variations of the T_g , determined by the penetration method, are shown in Fig. 2. When MEK is used, the observed T_g deviates significantly from ideal mixing behaviour. Similar experiments were performed, starting with solvent having compositions of 1:1, 3:2 and 7:3 w/w IPA–MEK. The polymer was equilibrated with the solvent for two days at 40 °C and then the samples were measured. The following observations were made.

1:1 w/w IPA–MEK/PMMA mixtures. At room temperature, for 60 to 90% solvent to polymer mixtures, not all of the added solvent was absorbed. Below 60%, all the solvent was absorbed and the solid was clear. Below 0 °C, the excess solvent is cloudy in the 90 to 80% samples, but is clear in the 70 and 60% samples. For 90 to 40% samples, there is a double layer visible in the polymer layer. The lower part of the solid is clear. However, the upper layer is opaque. On cooling, the 30 to 20% samples remain unchanged.

3:2 w/w IPA–MEK/PMMA mixtures. Two phase behaviour is visible at room temperature for the 90 to 40% solvent to polymer mixtures. The excess solvent is clear at room temperature, but cloudy below 0 °C.

7:3 w/w IPA–MEK/PMMA mixtures. At 40 °C, the polymer mixtures are clear in most cases. The exception is that in the 90 to 60% solvent to polymer mixtures, there is a surface layer of opaque polymer. Excess solvent is evident in the 90 to 40% samples. At room temperature, two phase behaviour is evident

in samples 90 to 30%, with the excess solvent becoming cloudy in the 90 to 70% samples.

The penetration technique was used to measure the solids which contained various levels of absorbed solvent. The results are presented in Fig. 2. It is evident that the T_p , which is closely associated with the T_g , has essentially the value expected for depressions produced by MEK for low values of polymer to solvent, and it is only at higher values of solvent absorption that deviations from the 'ideal MEK' curve are observed. The values of T_p are very close to those of the T_g measured previously on bulk samples.²¹ The liquid layer was analysed using ¹H NMR signal intensities to determine its compositions (Table 1). Analysis of the composition of the excess liquid layer shows that, for solutions with low solids content, the solution composition is identical to that of the solution. However, as the volume of solvent in the polymer mixture is reduced, the good solvent is preferentially absorbed leading to changes in the measured composition compared with that originally used to produce the mixture. This implies that, at any point during the diffusion process, the composition can deviate from that of the contacting mixture as a consequence of preferential absorption of MEK. The average mutual diffusion coefficient must therefore be considered as reflecting the overall behaviour of the system and incorporates the effects of the precipitation as well as solubility–diffusion.

Effect of glass transition temperature on the diffusion behaviour

The spun polymer resist is usually baked at a temperature above the T_p before being exposed to electron beam irradiation. The process is carried out to increase the mechanical rigidity, flatness of the film and to improve the development characteristics, after electron beam exposure. For PMMA, baking is usually performed at between 130 and 160 °C for 1 h. Not all of the residual casting solvent is removed during the

Table 1 Variation in the composition with the volume of solvent added for various starting compositions of MEK and IPA

Solvent added (%)	Solvent absorbed (%)	IPA in solvent residue (%)	Solvent added (%)	Solvent absorbed (%)	IPA in solvent residue (%)
<i>1:1 w/w IPA–MEK</i>					
90	56	55	80	53	55
70	55	57	60	55	60
50	50	61	40	40	no residual
30	30	no residual	20	20	no residual
<i>3:2 w/w IPA–MEK</i>					
90	55	62	80	53	64
70	51	64	60	49	71
50	49	no residual	40	39	no residual
30	30	no residual	20	20	no residual
<i>7:3 w/w IPA–MEK</i>					
90	54	71	80	45	76
70	46	77	60	46	80
50	42	78	40	40	77
30	30	no residual	20	20	no residual

Table 2 Description of the PMMA films used in the study of the effects of T_g on the mutual diffusion coefficients

Film	Initial T_g /°C	Thermal–time treatment	Final T_g /°C
A	66	7 days @ ambient T and P	73
B	59	12 days @ ambient T and P and 24 h in a vacuum oven at ambient T	78
C	61	vacuum oven; 40 °C/48 h, 60 °C/24 h, 80 °C/36 h	98
D	60	ambient P , 130 °C/1 h	106
E	64	ambient P , 160 °C/1 h, cooled straight from oven	112
F	61	ambient P , 160 °C/1 h, cooled very slowly over 24 h	110

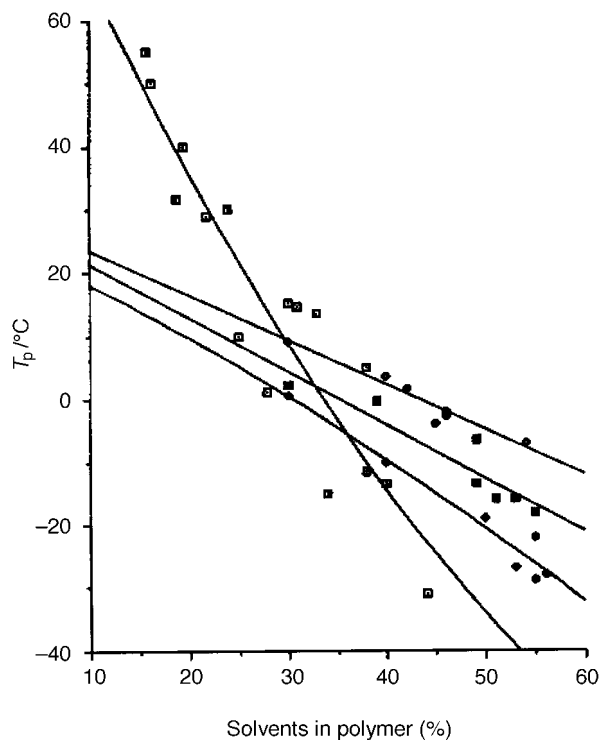


Fig. 2 Variation of the penetration temperature (T_p) for various IPA-MEK mixtures with PMMA: (\square) pure and (\blacklozenge) 1:1, (\blacksquare) 3:2 and (\diamond) 7:3 MEK, w/w IPA-MEK. The errors in the experimental points are ± 3 K; the lines are guides to the data.

spinning process and it is appropriate to examine the effects of T_p and, hence, the residual solvent content on the development/diffusion behaviour.

A series of films was produced by casting. Their initial values of T_p are presented in Table 2. These low T_p films which contain residual casting solvent will slowly lose solvent and increase their T_p at a rate of approximately 1°C per day. Measurements were performed within 2 h of the T_p measurements. The values quoted in Table 2 are, therefore, the values of the films used in the diffusion study. Since the diffusion cell is a sandwich of heavy glass plates, further significant loss of solvent is unlikely once the cell has been constructed.

Film A ($T_p = 73^\circ\text{C}$). The concentration-distance profiles for the exposure of the films to three different solvent compositions are shown in Fig. 3(a). The plot for the 1:1 w/w IPA-MEK mixture is sigmoidal in shape and $\phi_s = 0.5$ when $x/\sqrt{t} = 0$, indicating that the rate of solvent penetration into the film is equal to the rate of polymer dissolution into the solvent and that simple Fickian diffusion is observed. Consistent with this assumption is the disappearance of the film edge after about 8 min of exposure to solvent. For the 3:2 w/w IPA-MEK mixture, there is a discontinuity at $\phi_s = 0.8$, indicating that the solvent mixture is no longer able to dissolve the polymer completely. The behaviour of the 7:3 w/w IPA-MEK solutions is similar to that of the 3:2 w/w IPA-MEK mixture, except that it shows less penetration of solvent into the polymer and less swelling. The calculated mutual diffusion coefficient-concentration curves [Fig. 3(b)] show almost symmetrical behaviour, the curves for the 3:2 and 7:3 w/w IPA-MEK mixtures being truncated, reflecting swelling without dissolution of the polymer in the solvent.

Film B ($T_p = 78^\circ\text{C}$). From studies of 1:1 w/w IPA-MEK mixtures, the concentration-distance curves indicate, once more, approximately sigmoidal behaviour, with the disappearance of the film edge after 9 min [Fig. 4(a)]. For the 3:2 and

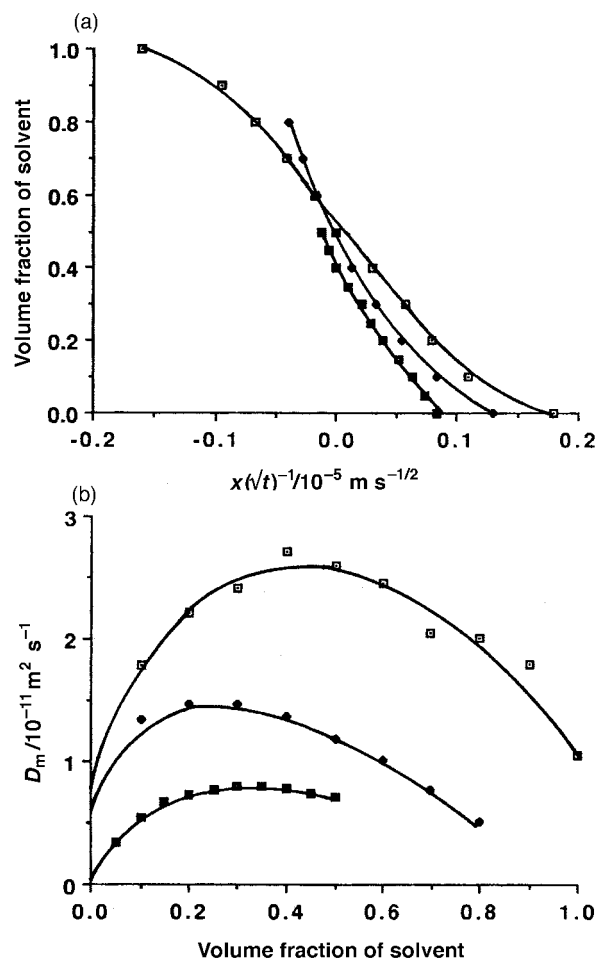


Fig. 3 Boltzmann transformation curves. (a) Volume fraction of solvent versus distance/ $\sqrt{\text{time}}$ for film A. (b) Mutual diffusion coefficients for different solvent mixtures for film A. (\square) 1:1, (\blacklozenge) 3:2 and (\blacksquare) 7:3 w/w IPA-MEK. The errors are estimated to be ± 0.05 in the volume fraction in (a) and $\pm 0.05 \times 10^{-11} \text{ m}^2 \text{ s}^{-1}$ for each data point in D_m in (b).

7:3 w/w IPA-MEK mixtures, the curves are crescent shaped and truncated at $\phi_s = 0.7$ and $\phi_s = 0.5$ respectively. The curves are almost indistinguishable up to $\phi_s = 0.5$ and, as a consequence, the mutual diffusion curves [Fig. 4(b)] are essentially identical.

Film C ($T_p = 98^\circ\text{C}$). The composition-distance curves obtained with the three solvent mixtures are shown in Fig. 5(a). In the case of the 1:1 w/w IPA-MEK mixtures, the film edge disappears after 25 min and recedes as dissolution takes place. The 3:2 w/w IPA-MEK mixture relationship is again sigmoidal in behaviour and extends up to $\phi_s = 1.0$. The edge is not well defined and abrupt kinks in the fringe pattern are observed rather than a distinct discontinuity. In the case of the 7:3 w/w IPA-MEK mixture, a secondary boundary was evident even after 120 min. The diffusion coefficients for the lower concentrations are shown in Fig. 5(b).

Film D ($T_p = 106^\circ\text{C}$). The concentration-distance curves for two of the mixtures are shown in Fig. 6(a). As with film C, the shapes of the curves are similar to those observed for other films. A distinct edge receding with time was observed after 16 min. This edge quickly disappears as dissolution of the polymer takes place. In the case of the 7:3 w/w IPA-MEK mixture, it was not possible to calculate curves as the films exhibited both environmental stress cracking and also the presence of a secondary boundary.

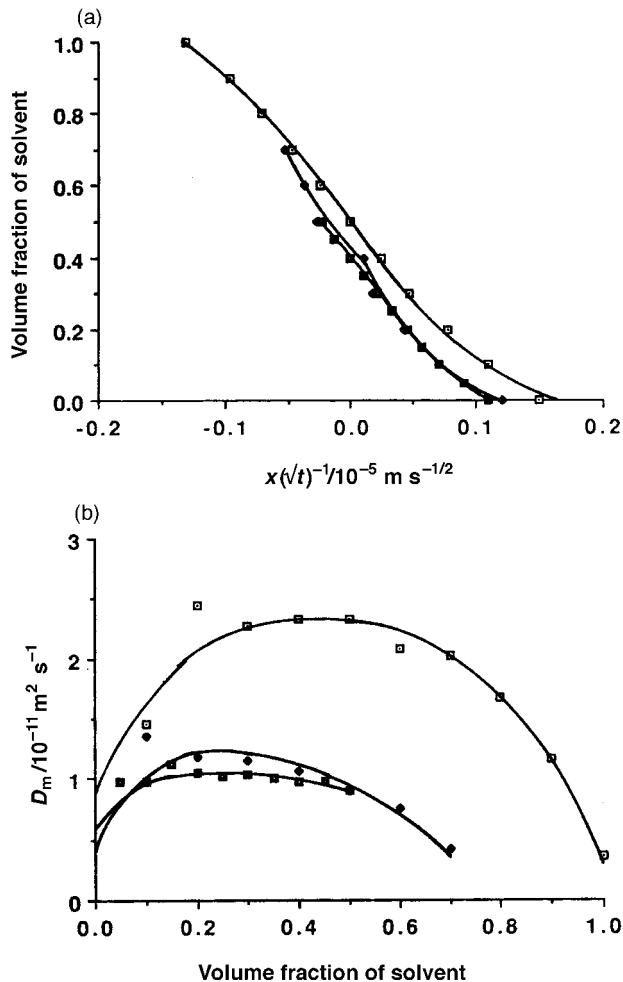


Fig. 4 Boltzmann transformation curves. (a) Volume fraction of solvent versus distance/ $\sqrt{\text{time}}$ for film B. (b) Mutual diffusion coefficients for different solvent mixtures for film B. (\square) 1:1, (\blacklozenge) 3:2 and (\blacksquare) 7:3 w/w IPA–MEK. The errors are estimated to be ± 0.08 in the volume fraction in (a) and $\pm 0.1 \times 10^{-11} \text{ m}^2 \text{ s}^{-1}$ for each data point in D_m in (b).

Film E ($T_p = 112^\circ \text{C}$) and film F ($T_p = 110^\circ \text{C}$). Film F would be expected to have a lower residual solvent content as it was kept at a higher temperature for a longer period of time. In both cases, environmental stress cracking made analysis of the diffusion behaviour very difficult. In both cases, the film edge receded with time as dissolution of the polymer molecules into the solvent occurred. The film edge disappeared after a period of about 27 min for film E and after 100 min for film F. Stress cracking is a consequence of the osmotic pressure increasing quickly in the film edge and the polymer behind being unable to release the stress which is generated.

Comparison of the data from the various films exposed to the 1:1 w/w IPA–MEK indicates that all the curves are virtually superimposable, with only slight differences, in the region $\phi_s = 0.7\text{--}1.0$ and in the range $\phi_s = 0\text{--}0.3$, being observed (Table 3). There is a marked decrease in D_m as the solvent mixture is changed from 1:1 to 7:3 w/w IPA–MEK, this effect being particularly marked for the low T_p film. There is slight reduction in the diffusion coefficient with increase in the T_p . However, this effect is not as marked as the solvent effect. There are no data presented for films C and D for 7:3 w/w IPA–MEK as these exhibited marked crazing. As the composition of the solvent mixture is changed, the plots of D_m against ϕ_s become asymmetric towards low values of ϕ_s .

The polymer chains will be extended in the good solvent used for spin casting the films and this extended structure, as a consequence of chain entanglement, will be retained in the

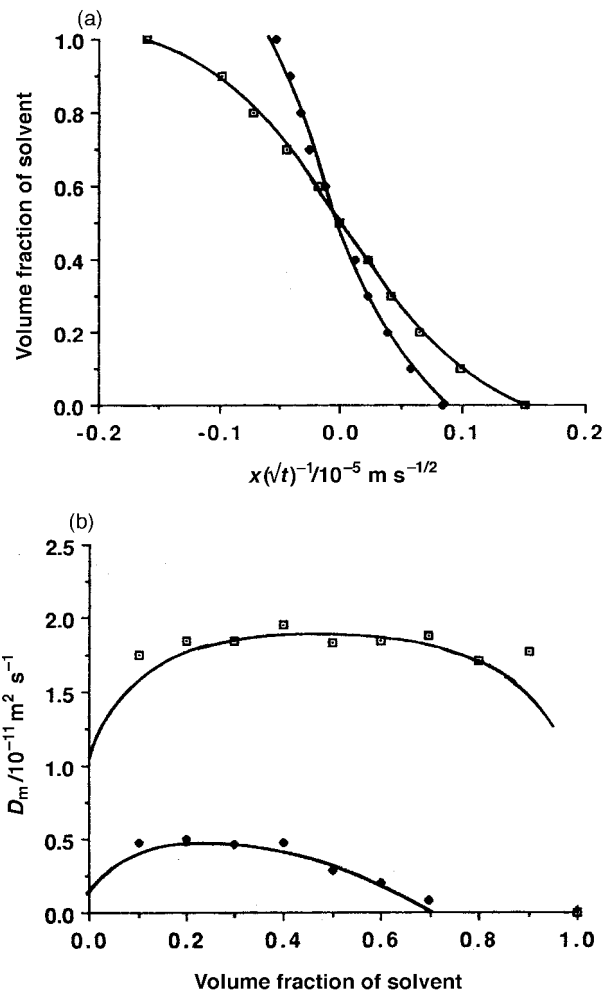


Fig. 5 Boltzmann transformation curves. (a) Volume fraction of solvent versus distance/ $\sqrt{\text{time}}$ for film C. (b) Mutual diffusion coefficients for different solvent mixtures for film C. (\square) 1:1, (\blacklozenge) 3:2 and (\blacksquare) 7:3 w/w IPA–MEK. The errors are estimated to be ± 0.05 in the volume fraction in (a) and $\pm 0.15 \times 10^{-11} \text{ m}^2 \text{ s}^{-1}$ for each data point in D_m in (b).

solid state. The non-equilibrium chain structure will attempt to gain its equilibrium state as the film is swollen and, hence, will generate stresses that may lead to stress crazing. The removal of solvent will be accompanied by generation of denser, more compact structures and a concomitant reduction in the diffusion coefficient would be observed. The apparently anomalous behaviour of the 106°C film can be explained by the fact that, in this case, contact with poor solvent allows re-dissolution of the polymer molecules in the surface without significant re-swelling of the molecules that form the bulk of the material. Hence, the rate of dissolution of the polymer becomes comparable to the rate of solvent penetration into the polymer and crazing is not observed.

Swelling behaviour

The development process is a combination of dissolution and swelling of the polymer matrix. The swelling rate can be measured directly from the movement of the solvent polymer interface, obtained from the interferograms. Change in the T_p of the films leads to small changes in the swelling rate with the 3:2 w/w IPA–MEK (Fig. 7). There are two effects which need to be considered in interpretation of these data. Firstly, the polymer films are obtained from a good solvent. Also, it is probable that the polymer molecules may have retained their expanded conformations with the possible effect of micro-crazing at the surface in the higher T_p films influencing the

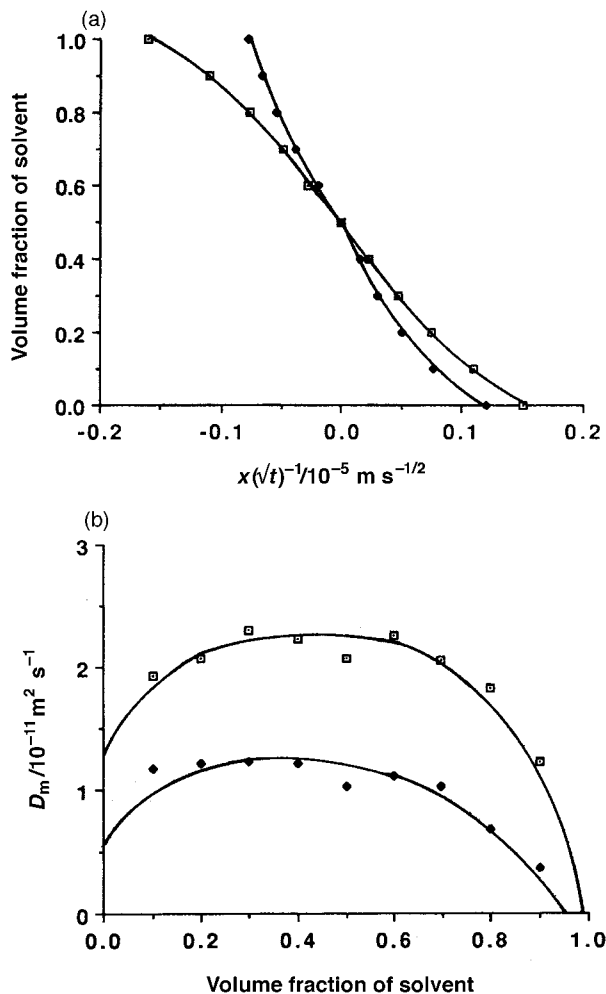


Fig. 6 Boltzmann transformation curves. (a) Volume fraction of solvent versus distance/ $\sqrt{\text{time}}$ for film D. (b) Mutual diffusion coefficients for different solvent mixtures for film D. (□) 1:1 and (◆) 3:2 w/w IPA-MEK. The errors are estimated to be ± 0.05 in the volume fraction in (a) and $\pm 0.1 \times 10^{-11} \text{ m}^2 \text{ s}^{-1}$ for each data point in D_m in (b). The errors at the extremes of the curves are greater than the average values.

Table 3 Mutual diffusion coefficients for films with different values of T_g

IPA %	$D_m \text{ (max)}/10^{-10} \text{ m}^2 \text{ s}^{-1}$			
	Film A	Film B	Film C	Film D
50	0.26	0.23	0.20	0.22
60	0.14	0.13	0.05	0.12
70	0.08	0.11	—	—

initial diffusion behaviour. Secondly, there are marked differences in the swelling rate with change in solvent.

Conclusions

Change in the composition of the solvent mixture used in the measurement of the mutual diffusion coefficient for PMMA films has significant effects on the T_p of the film. The higher the T_p of the films formed after baking, the more susceptible are the films to crazing. In the resist development process, crazing probably plays an important role as dissolution in the overall process. The diffusion of the solvent into the polymer film is a complex process which involves selective diffusion of the better solvent, lowering the T_p of the films

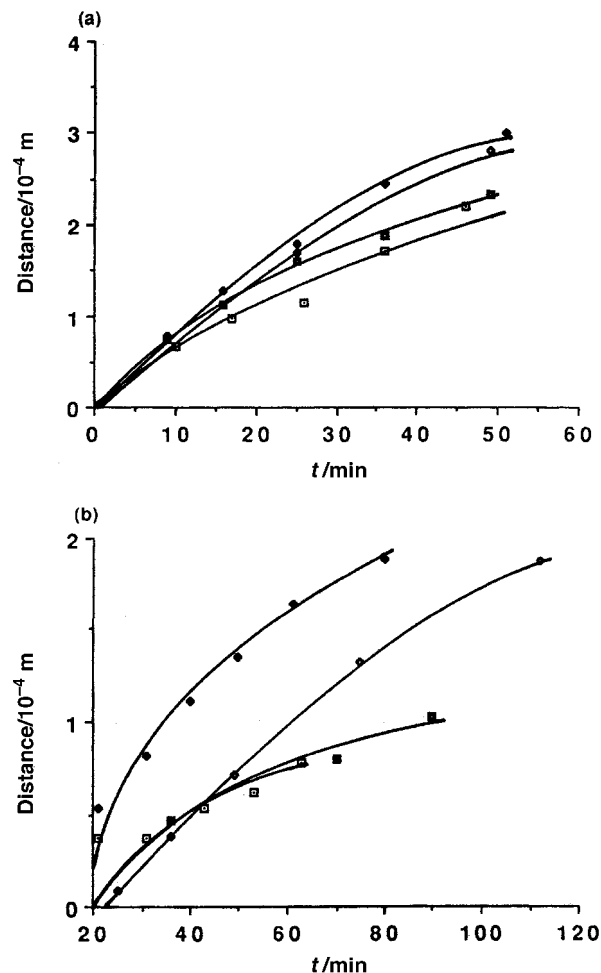


Fig. 7 Swelling rate curves for (a) 3:2 and (b) 7:3 w/w IPA-MEK. (□) Film A, (◆) film B, (■) film C and (◇) film D. The errors in the distances are of the order of 0.1×10^{-4} .

and precipitation of polymer in the swollen layer by the poorer solvent.

Acknowledgement

One of the authors (K.E.R.) wishes to acknowledge the support of the EPSRC in provision of support in the form of a studentship for the period of this study.

References

- 1 P. C. Tsiartas, L. W. C. L. Henderson, W. D. Hinsberg, I. C. Sanchez, R. T. Bonnecaze and C. Grant Willson, *Macromolecules*, 1997, **30**, 4656.
- 2 J. M. D. McElroy, *Diffusion in Polymers*, ed. P. Neogi, Marcel Dekker, New York, Basel, Hong Kong, 1996, p. 1.
- 3 J. Crank, *The Mathematics of Diffusion*, Oxford, 1985, p. 256.
- 4 N. A. Peppas, J. C. Wu and E. D. von Meerweil, *Macromolecules*, 1994, **27**, 5626.
- 5 P. G. de Gennes, *Scaling Concepts in Polymer Physics*, Cornell University Press, Ithaca, NY, 1979.
- 6 A. C. Ouano and J. A. Carothers, *Science and Technology of Polymer Processing*, ed. N. P. Sung and N. H. Sung, MIT Press, Cambridge, MA, 1979, p. 755.
- 7 A. C. Ouano and J. A. Carothers, *Structure-Solubility Relationships in Polymers*, ed. F. W. Harris and R. B. Seymour, Academic Press, New York, 1977, p. 11.
- 8 A. C. Ouano, Y. O. Tu and J. A. Carothers, *Polym. Prepr.*, 1976, **17**, 329.
- 9 A. C. Ouano, *Polymers in Electronics*, ed. T. Davidson, *ACS Symp. Ser.*, 1984, **242**, 84.

- 10 R. A. Pethrick, *Irradiation Effects on Polymers*, ed. D. W. Clegg and A. A. Collyer, Elsevier Applied Science, London, 1991, p. 403.
- 11 V. K. Sharma, R. A. Pethrick and S. Affrossman, *Polymer*, 1982, **23**, 1732.
- 12 T. Kato, *Microelectronic Polymers*, ed. M. S. Htoo, Marcel Dekker, New York, 1989, p. 1199.
- 13 M. M. O'Toole, *Microelectronic Polymers*, ed. M. S. Htoo, Marcel Dekker, New York, 1989, p. 315.
- 14 M. J. Bowden, *Materials for Microlithography*, *ACS Symp. Ser.*, 1984, **266**, 71.
- 15 L. F. Thompson, *Introduction to Microlithography*, 2nd edn., ed. L. F. Thompson, C. Grant Willson and M. J. Bowden, ACS Professional Reference Books, ACS, Washington DC, 1994, p. 280.
- 16 K. E. Rankin and R. A. Pethrick, *Microelectron. Eng.*, 1995, **26**, 141.
- 17 K. R. Dunham, *Solid State Technol.*, 1971, **14**(6), 41.
- 18 J. Crank, *The Mathematics of Diffusion*, Oxford Science Publications, Oxford, 1985, p. 230.
- 19 J. Crank and G. S. Park, *Diffusion in Polymers*, ed. J. Crank and G. S. Park, Academic Press, New York, 1968, ch. 1, p. 4.
- 20 J. Crank and C. Robinson, *Proc. R. Soc. London, Ser. A*, 1951, **204**, 549.
- 21 R. J. Elwell, D. Hayward and R. A. Pethrick, *Polym. Int.*, 1993, **30**, 55.

Paper 8/02466I